High strength metakaolin-based geopolymer reinforced by pristine and covalent functionalized carbon nanotubes

Wassila Sekkal, Ali Zaoui

High strength metakaolin-based geopolymer reinforced by pristine and covalent functionalized carbon nanotubes

W. Sekkal and A. Zaoui*

Univ. Lille, IMT Lille Douai, Univ. Artois, JUNIA, ULR 4515 - LGCgE, Laboratoire de Génie Civil et géo-Environnement, F-59000 Lille, France

Abstract

The present work provides new insight into the effects of pristine and functionalized carbon nanotubes (CNT's) on the mechanical properties of metakaolin-based geopolymer nanocomposites. Single pristine CNT's and doped CNT-oxide are added to the geopolymer paste at concentrations varying from 0 to 8.31 wt % and from 0 to 10 %, respectively. Reactive molecular dynamics calculations reveal that the mechanical properties of oxide carbon nanotubes deteriorate since covalent bonds created through C-OH interaction lead to defects creation converting their surface SP^2 hybridation to SP^3. However, they make the structure denser and improve the mobility of CNT's into the matrix. Results show that the diffusion coefficient of CNT-oxide in geopolymer matrix is three times the one of pristine CNT. The tensile tests reveal that the incorporation of a low content of 1.08 wt.% pristine CNT increases the elastic and the indentation modulus up to 74% and 94%, respectively. However, for higher concentration, both properties drop with increasing CNT concentration. The addition of 10% doped CNT-oxide leads to a raise of elastic modulus and bulk density by 165% and 22.5%, respectively.

* Corresponding author: Tel: 0033 6226 8976. E-mail: **azaoui@polytech-lille.fr (Ali Zaoui)**

1. Introduction

Developing a higher-strength geopolymer material is a great challenge in civil engineering, offering a new generation of building and construction materials with better mechanical properties, lower shrinkage and superior durability as well as environmental sustainability. A promising way to achieve this development is the incorporation of nanomaterials, which minimizes the air gaps content in the nanostructure and allows for a non-corrosive reinforcement. The denser microstructure positively affects the physical and mechanical properties of the novel nanocomposite. Researchers attempt to incorporate different nanofillers to enhance the performance of geopolymer materials. Xie and Fang[1], and Sumesh et al.[2] reviewed the modification of geopolymer composites properties with nanomaterials and underline that most attention was paid to the influence of nano-SiO_2, nano-Al_2O_3, nano-TiO_2, nano-Fe_2O_3, and nano-clay. Experimental SEM tests reveal that the addition of 6% of nano-SiO_2 leads to the improvement in compressive, flexural and tensile strength at 28 days under ambient temperature curing[3]. The work of Phoo-ngernkham et al.[2] shows that the incorporation of 2% of nano-silica and 1% of nano-alumina cured for 90 days, gives the compressive strength of 51.8 and 56.4 MPa, respectively[4]. Of late years, research on the addition of carbon-based nanomaterials in geopolymers has drawn research attentions[5-10]. Particularly, carbon nanotubes (CNT's) are expected to be excellent candidates and innovative reinforcements due to their superior mechanical properties[11]. However, the main prerequisites that determine the performance of the CNT/geopolymer are the good dispersion[12-15]. In fact, due to the highly attractive van der Waals forces, CNT tend to remain agglomerated, which causes the decrease of the performance of composites[16-19]. To date, extensive research is made on the study of the mechanical enhancement of CNT on geopolymer. Abbasi et al.[14] reported that the addition of only 0.5 wt% Multi-Walls CNT (MWCNT) on fly ash leads an increase of flexural strength and elastic modulus by 128% and 109%, respectively. On the other hand, the experimental work of Saafi et al.[19] showed that the addition of MWCNTs increased the flexural strength, Young's modulus and flexural toughness by 160%, 109% and 275%, respectively. It also enhanced the fracture energy and increased the electrical conductivity by 194%. Luz et al.[20] observed that the addition of 0.1 wt% of pristine CNT in metakaolin geopolymer leads improvements of 3.8%, 13.2% and 28.7% in the Young's modulus, compressive and flexural strengths, respectively. Nevertheless, an increase of about 10.2% in the porosity is obtained when the dosage of CNT exceeds 0.2 wt% inducing to a decrease of 3.5%, 11.8% and 31.0%, for Young modulus, compressive and flexural strengths, respectively. Yuan et al.[21] reported that 3 wt% of COOH-

multi-walled CNT enhances the flexural strength, the elastic modulus and the fracture toughness within 42.3%, 29.6% and 38.5%, respectively. Moreover, it is found that the inclusion of graphene and its derivatives such as graphene oxide and reduced graphene oxide lead to interesting properties [22]. Zhang et al.[23] studied the substitutional doping of graphene with silicon incorporated in metakaolin geopolymer using reactive molecular dynamics simulations. Their obtained results show that the elastic modulus of 10% Si-graphene/geopolymer is double than graphene/geopolymer matrix. Besides, the dispersion problem encountered during the CNT reinforcement ad interfacial chemical bonding have also a great impact on the structure and mechanical properties of the reinforced nanocomposite, as reported in some works[24-25].

Though all research is promising, more efforts are deemed necessary essentially in modeling and simulation to bridge the gaps with experimental findings. Only two works have been done on atomistic simulation of the reinforcement of geopolymers through the incorporation of carbon-based materials[23, 26]. In these two studies[23, 26], authors fixed the concentration of Si-doped graphene and CNT to be around 6 wt%. According to all experimental measurements[3-21] performed in that subject, the dosage of incorporated nanomaterials is of great importance and affects considerably the mechanical properties of reinforced geopolymers. Therefore the main novelty of this work compared to previous studies [23,26] is that we consider for the first time the incorporation of CNT nanofillers with a dosage varying from 0 to 8.31 wt%. We will focus on elucidating the effect of pristine and covalent functionalized CNT on the mechanical properties of metakaolin geopolymer. Based on molecular dynamics simulation and using a reactive force field, we aim mainly to find the optimum dosage for CNT that enhances the elastic response of CNT/geopolymer nanocomposite. Moreover, the role of functionalized CNT on the improvement of their mobility and the stability of the nanostructure is also discussed.

2. Molecular modeling and force fields

According to Davidovidts[27, 28], creating geopolymer paste requires alumina silicate material (metakaolin, fly ash, etc.), alkaline reagent (sodium or potassium soluble) and water. In the first step of polymerization, the dissolution of aluminosilicate source in the alkali solution leads to the formation of Al-OH and Si-OH bonds[29]. After the hydrolysis process, $Al(OH)_4$ and $Si(OH)_4$ are released and then polymerized to form aluminosilicate oligomers[30-31]. Finally the condensation reactions produce a crosslinked 3D network structure from which we can class mainly three types of structures depending on Si/Al ratio: sialate (Si/Al = 1), sialate-

siloxo (Si/Al=2), and sialate-disiloxo (Si/Al = 3). In the present study, we use sialate-disiloxo oligomers (Si/Al = 3) ($NaAlSi_3O_{13}$) to represent the geopolymer structure. The preparation of CNT/geopolymer model evolves the following steps: first a supercell with a size of 8x 8 x 8 nm is built where (6,6) CNT molecules with various concentrations (0 – 8.31 wt%) are dispersed randomly. Then 1601 oligomers are packed into the box within water molecules so that the water content in the nanostructure is fixed to 7.7 wt.%, as reported in the work of Zhang et al.[32]. The density of the system is equal to 2 g/cm^3 leading to a model nanostructure of 38361 atoms. The chemical composition of metakaolin geopolymer model is presented in Table 1. A side view the CNT/geopolymer model with 3.73 wt% CNT concentration is presented in Fig.1. In the present study, pristine and CNT-oxide molecules are used within various hydroxyl groups attached to randomly carbon atoms, as presented in Fig.2. The CNT-oxide concentrations are equal to 0% (pristine CNT), 2.5%, 5%, 7.5% and 10% (Fig.2b).

In this study, Reactive force filed (ReaxFF), developed by van Duin et al.[33] is carried out to represent the interatomic interactions in the CNT/geopolymer model. It is a bond-order dependent potential where the atomic charges are calculated from its charge equilibration nature, which makes it possible to simulate chemical reactions. The bond order is directly calculated from the instantaneous distances that are updated systematically allowing the creation and dissociation of bonds during simulation. The total energy (E_{Tot}) of a system, as described in equation (1), is of a sum of several energies: the bond formation energy (□□□□□), the van der Waals energy (□□□□), the Coulombic contribution (□□□□□), the angular and torsional energy (□□□□, □□□□), the lone pair energy (□$_{lp}$) and finally the energy penalty for under/over coordination stability of atoms (□□□□□□, □□□□□):

□$_{Tot}$ = □□□□□ + □□□□ + □□□□□ + □□□□ + □□□□ + □$_{lp}$ + □□□□□□ + □□□□□ (1)

The ReaxFF forcefield has been applied successfully on geopolymer[23], calcium silicate hydrates[34], sodium aluminosilicate glass[35,36], silica[37,38], zeolite[39,40] and clay minerals[41,42].

3. Simulation procedure

The CNT/geopolymer model, as presented in section II, is first relaxed based on the conjugate gradient algorithm with a convergence criterion of 10^{-12} kcal/mol to optimize the system geometry. Then molecular dynamics simulations are performed to equilibrate the system under an NVT ensemble for 100 ps at 300 K using a time step of 0.2 fs. After, a heating is

applied up to 2000K for 100 ps using a timestep of 0.2fs in NPT ensemble, followed by quenching to 300K with a cooling rate of 1 K/ps to realize the polymerization of oligomer and thus produce a cross-linked geopolymer matrix. The obtained structure is then relaxed in the *NPT* ensemble for 200 ps at 300K. Periodic boundary conditions are applied to all directions during the simulation procedure. Further equilibration for 1ns is performed to compute the trajectory information of atoms in order to study the dynamical properties of the nanostructure. A constant strain method is employed to calculate the mechanical properties where a series of expansions at 0.0001/ps are applied to the supercell.

4. Results and discussion

4. 1. Effect of pristine CNT content on the mechanical properties of geopolymer nanocomposite

Since their discovery, carbon nanotubes have aroused the interest of researchers as composite reinforcements and weight reducers thanks to their high elastic modulus of ~ 1 TPa[43]. The main concern of this section is to address the role of pristine CNT in reinforcing the geopolymer nanostructure. The tensile processes are investigated by using the constant-strain method to assess the elastic and indentation modulus of the CNT/geopolymer nanocomposites with various CNT concentrations from 0.0 to 8.31 wt%. First, the obtained elastic modulus for plain geopolymer model is found to be equal to 46.21 GPa, in agreement with the obtained values of 45.1 GPa[23] and 42 GPa[44]. Figures 3 and 4 depict the obtained data of the elastic and the indentation modulus for various CNT concentrations. The data in Fig. 4 are compared to experimental measurements[45] for only low CNT content and seems to be in agreement with our results. It is noticed for both figures that the highest mechanical improvement is achieved at CNT concentration of 1.08 wt%, with the elastic and indentation modulus increase of 74% and 93.4%, respectively. Higher CNT dosage leads to a gradually strength decrease, due to the highly attractive van der Waals forces between CNT caused by the high specific surface area of CNT. This phenomenon will lead to the agglomeration of CNT, which makes the dispersion problematic since it causes and a decrease of bonding between geopolymer and CNT and hence affects the strength and the mechanical performance of the system. Using a multi-stage hierarchical micromechanical model Hasanzadeh et al.[46] show that the CNT agglomeration influences and degrades considerably the creep resistance of the CNT-polymer system. It is also found that the interphase region affects mainly the effective properties of the piezoelectric hybrid composites [47].

Besides, it is observed particularly that the addition of 8.31 wt% of CNT results to an elastic modulus value of 45.59 GPa close to the value for the plain geopolymer (46.21 GPa). Our results are in agreement with experimental work of Jittabut et al.[48] on reinforcing ash fly geopolymer using CNT dosage from 1 to 5 % by weigth. They found that the optimum of 1 wt% carbon nanotubes addition exhibited the highest strength increase (32%). Saafi et al.[19] studied the effect of multiwalled carbon nanotubes (MWCNT) on fly ash geopolymeric composites with very low concentrations (0.1%, 0.5%, 1%). Their experimental results showed the enhancement of flexural strength, flexural toughness and Young's modulus is 128%, 207% and 109%, respectively at 0.5 wt% CNT content. On the other hand, Abbasi et al.[14] found that the addition of 0.5 wt% MWCNT increases the Young modulus and the flexural strength by 109% and 128%, respectively.

The bulk densities of CNT/geopolymer nanostructure are calculated for various CNT concentrations, as shown in Fig.5. The results follow the same tendency as for the mechanical findings since an optimum value of the bulk density is obtained for the sample with 1.08 wt% of CNT addition. For higher concentrations, the bulk densities values decrease but they remain higher than the plain geopolymer's data. The study of the interfacial energy variation with CNT content, as presented in Fig.6, proves the stability of the nanostructure at 1.08 wt% concentration since the obtained energy is the lowest one. Therefore, it can be seen that the incorporation of low content of pristine CNT has a beneficial effect on condensing the metakaolin geopolymer nanocomposite and enhancing the corresponding mechanical properties.

4.2. Effect of functionalized CNT

Our results as well as experimental studies[14, 20] show a strength loss when CNT concentration surpasses an optimum amount. This behavior is due to the agglomeration of CNT leading a difficulty in uniformly dispersing CNT in geopolymer matrix. Luz et al.[20] reported that no threshold was observed for functionalized CNT compared to pristine CNT. In this section our aim is to study the variation of structural and elastic properties with covalent functionalized CNT concentrations. As presented in Fig.2b, CNT-oxide molecules are used within hydroxyl groups attached to randomly carbon atoms. The CNT-oxide doping concentrations are equal to 2.5%, 5%, 7.5% and 10%. This functional group improves CNT dispersion and provides a larger number of active sites for connection with geopolymer matrix. First, we address in Fig. 7 the variation of Elastic modulus of carbon nanotubes with OH concentrations. Compared with pristine CNT, CNT-oxide has lower elastic modulus since covalent bonds created

through C-OH interaction lead to defects creation converting their surface SP^2 hybridation to SP^3 [49-51]. At OH concentration of 10%, CNT-oxide loose about 25% in the elastic modulus. Zhang et al. [23] reported also that the graphene oxide and Si-graphene (doping concentration of 10%,) show losses in the elastic modulus of about 9.9 and 43.3%, respectively. However, as the elastic properties of Si-graphene and in our case CNT-oxide are much higher than that of geopolymer structure, they found that such nanofillers possess a great potential to reinforce geopolymer composite.

In the following, calculations have been carried out in a supercell with a size of 3.5 x 3.5 x 5.5 nm containing one (6,6) CNT-oxide representing 6 wt% of CNT content in the nanostructure (Fig.8). We have chosen this value in order to compare our results with those of Zhang et al.[23] using graphene oxide and Si-doped graphene with a concentration of about 6 wt%. Fig. 9 represents the variation of the mean and the transversal elastic modulus data with OH concentrations, compared to the reactive molecular dynamics calculations of Zhang et al.[23]. It is observed that the mean young modulus increases with increasing C-OH concentration. The obtained value at 10% C-OH is 2.65 times higher than the one obtained in the case of pristine CNT due to the chemically bonded interface. The main enhancement comes from the transversal elastic response of the nanostructure, as appeared in Fig.9. Moreover, one may observe that incorporating CNT-oxide (with 10% C-OH concentration) into geopolymer structure leads to a higher enhancement of the elastic modulus (165%) comparing to 65% in the case of 10% Si-doping graphene [23]. Moreover, it is found that the addition of 10% Si-graphene[23], Young's modulus is enhanced by 64.2%. Fig. 10 illustrates the increase of the bulk density of CNT-oxide/geopolymer with C-OH concentration. That means that the nanostructure becomes denser for higher OH concentrations since the obtained raise is of 22.5% at 10% C-OH concentration.

4.3. Diffusion of CNT in geopolymer nanocomposites

With the aim of understanding the mobility of CNT in geopolymer matrix, we study in this section the effect of covalent functionalization of CNT (10% C-OH) on the dynamical properties of the nanostructure. Mean square displacement (*MSD*) and self-diffusion coefficient (*D*) are analyzed for CNT atoms and Na^+ cations for comparison, as presented in the following equations:

$$MSD(t) = \langle |r_i(t) - r_i(0)|^2 \rangle \quad (2)$$

$$D = \frac{1}{6}\frac{MSD(t)}{t}$$

where $r_i\ (t)$ is the position of atom i at time t. As shown in Fig.11, MSD of CNT atoms and Na^+ cations are higher in the case of functionalized CNT incorporation. The obtained diffusion coefficients from the calculated slope according to equation (2) are reported in Table 2, in comparison with previous theoretical calculations[26]. The diffusion coefficient of CNT-oxide is found to be three times higher than the one of pristine CNT. This diffusive behavior of CNT-oxide is seen clearly in Fig.11a where a higher slope is observed. Besides, our results show that the mobility of Na^+ cations is equal to 0.376 x $10^{-11}$$m^2$/s in the case of the addition of pristine CNT to geopolymer matrix, in agreement with the calculated value of 0.345 10^{-1} m^2/s[26]. The functionalization of CNT leads to a rise of the diffusion of Na^+ cations by a factor of 3 since the obtained value is equal to 1.113 x 10^{-11} m^2/s.

5. Conclusion

The present work addresses the subject of the improvement of the mechanical properties of metakaolin geopolymer structure through the incorporation of CNT nanofillers with a dosage varying from 0 to 8.31 wt%. By means of reactive molecular dynamics simulation, our results demonstrates the presence of an optimum amount of pristine CNT (1.08 wt%) that enhance the elastic and the indentation modulus up to 74% and 94%, respectively. Tensile tests show that 10% doped CNT-oxide leads to a raise of the elastic modulus by 165% and makes the structure denser. Finally, it is observed that functionalized CNT improves the mobility of CNT in the matrix and makes the structure of geopolymer denser.

Acknowledgments

The authors would like to thank the French National Research Agency's (ANR) for the financial support of the "NanoGP" project under the number ANR-20-CE92-0016.

References:

[1] T.Y. Xie, C.F. Fang, Nanomaterials applied in modifications of geopolymer composites: a review, Aust. J. Civil Eng. 17 (2019) 32–49.

[2] M. Sumesh, U.J. Alengaram, M.Z. Jumaat, K.H. Mo, M.F. Alnahhal, Incorporation of nano-materials in cement composite and geopolymer based paste and mortar – a review, Constr. Build. Mater. 148 (2017) 62–84.

[3] D. Adak, M. Sarkar, S. Mandal, Constr. Build. Mater. 70 (2014) 453–459.

[4] P. Chindaprasirt, P. De Silva, K. Sagoe-Crentsil, S. Hanjitsuwan, s, J. Mater. Sci. 47 (2012) 4876–4883.

[5] S.J. Chen, F.G. Collins, A.J.N. Macleod, Z. Pan, W.H. Duan, C.M. Wang, Carbon nanotube–cement composites: a retrospect, ISE J. Part A: Civil Struct. Eng. 4 (2011) 254–265.

[6] H.B. Yang, H.Z. Cui, W.C. Tang, Z.J. Li, N.X. Han, F. Xing, A critical review on research progress of graphene/cement based composites, Compos. Part AAppl. S. 102 (2017) 273–296.

[7] Y.D. Xu, J.Q. Zeng, W. Chen, R.Y. Jin, B. Li, Z.H. Pan, A holistic review of cement composites reinforced with graphene oxide, Constr. Build. Mater. 171 (2018) 291–302.

[8] E. Shamsaei, F.B.D. Souza, X.P. Yao, E. Benhelal, A. Akbari, W.H. Duan, Graphene-based nanosheets for stronger and more durable concrete: a review, Constr. Build. Mater. 183 (2018) 642–660.

[9] B.G. Han, S.Q. Ding, J.L. Wang, J.P. Ou, Nano-Engineered Cementitious Composites: Principles and Practices, Springer, 2019.

[10] T.X. Huang, Z.Q. Sun, Advances in multifunctional graphene-geopolymer composite, Constr. Build. Mater., under review.

[11] N.J. Coleman, U. Khan, W.J. Blau, Y.K. Gun-ko, Small but strong: a review of the mechanical properties of carbon nanotube-polymer composites, Carbon 44 (2006) 1624–1652.

[12] G.M. Kim, I.W. Nam, B. Yang, H.N. Yoon, H.K. Lee, S. Park, Carbon nanotube (CNT) incorporated cementitious composites for functional construction materials: the state of the art, Compos. Struct. 227 (2019) 111244.

[13] H.M. Khater, H.A. Abd El Gawaad, Characterization of alkali activated geopolymer mortar doped with MWCNT, Constr. Build. Mater. 102 (2016) 329–337.

[14] S.M. Abbasi, H. Ahmadi, G. Khalaj, B. Ghasemi, Microstructure and mechanical properties of a metakaolinite-based geopolymer nanocomposite reinforced with carbon nanotubes, Ceram. Int. 42 (2016) 15171–15176.

[15] K.J.D. MacKenzie, M.J. Bolton, Electrical and mechanical properties of aluminosilicate

305 inorganic polymer composites with carbon nanotubes, J. Mater. Sci. 44 (2009) 2851–2857.
306 [16] E.T. Thostenson, Z. Ren, T.-W. Chou, Advances in the science and technology of carbon
307 nanotubes and their composites: a review, Compos. Sci. Technol. 61 (2001) 1899–1912.
308 [17] F. Sanchez, K. Sobolev, Nanotechnology in concrete–a review, Constr. Build. Mater. 24
309 (2010) 2060–2071.
310 [18] P.M. Ajayan, L.S. Schadler, P.V. Braun, Nanocomposite Science and Technology, John
311 Wiley & Sons, 2006.
312 [19]. M. Saafi, K. Andrew, P.L. Tang, D. McGhon, S. Taylor, M. Rahman, S.T. Yang, X. M.
313 Zhou, Multifunctional properties of carbon nanotube/fly ash geopolymeric nanocomposites,
314 Constr. Build. Mater. 49 (2013) 46–55.
315 [20] G. Luz, P.J.P. Gleize, E.R. Batiston, F. Pelisser, Effect of pristine and functionalized carbon
316 nanotubes on microstructural, rheological, and mechanical behaviors of metakaolin-based
317 geopolymer, Cem. Concr. Comp. 104 (2019) 103332.
318 [21] J.K. Yuan, P.G. He, D.C. Jia, S. Fu, Y. Zhang, X.Z. Liu, D.L. Cai, Z.H. Yang, X.M.
319 Duan, S.J. Wang, Y. Zhou, In situ processing of MWCNTs/leucite composites through
320 geopolymer precursor, J. Eur. Ceram. Soc. 37 (2017) 2219–2226.
321 [22] Q. Zheng, B. Han, X. Cui, X. Yu, J. Ou, Graphene-engineered cementitious composites:
322 Small makes a big impact, Nanomater. Nanotechnol. 7 (2017) 1–18,
323 https://doi.org/10.1177/1847980417742304.
324 [23] L.W. Zhang, M.F. Kai, X.H. Chen, Si-doped graphene in geopolymer: Its interfacial
325 chemical bonding, structure evolution and ultrastrong reinforcing ability, Cem. Concr.
326 Compos. 109 (2020), 103522, https://doi.org/10.1016/j. cemconcomp.2020.103522.
327 [24] J. Lu, M. Luo, B. I. Yakobson, Glass composites reinforced with silicon-doped carbon
328 nanotubes. Carbon 128, 231 (2018).
329 [25] Z. Wang, Q. Lv, S. Chen, C. Li, S. Sun and S. Hu, effect of interfacial bonding on
330 interphase properties in SiO_2/Epoxy nanocomposite: A molecular dynamics simulation study.
331 Acs Appl. Mater. Interfaces 8, 7499 (2016).
332 [26] M. Kai, L. Zhang, K. Liew, Carbon nanotube-geopolymer nanocomposites: a molecular
333 dynamics study of the influence of interfacial chemical bonding upon the structural and
334 mechanical properties, Carbon 161 (2020) 772–783.
335 [27]. Davidovits, J., Geopolymer Chemistry and Applications. 2008: Geopolymer Institute.
336 [28]. Davidovits, J. Properties of geopolymer cements. In First International Conference on
337 Alkaline Cements and Concretes. 1994.
338 [29] Z. Zuhua, Y. Xiao, Z. Huajun, C. Yue, Role of water in the synthesis of calcined kaolin-

based geopolymer, Appl. Clay Sci. 43 (2) (2009) 218–223.
[30] M. Abdullah, K. Hussin, M. Bnhussain, K. Ismail, W. Ibrahim, Mechanism and chemical reaction of fly ash geopolymer cement-a review, Int. J. Pure Appl. Sci. Technol. 6 (1) (2011) 35–44.
[31] P.S. Singh, M. Trigg, I. Burgar, T. Bastow, Geopolymer formation processes at room temperature studied by 29Si and 27Al MAS-NMR, Mater. Sci. Eng., A 396 (1–2) (2005) 392–402.
[32] Y. Zhang, J.L. Zhang, J.Y. Jiang, D.S. Hou, J.R. Zhang, The effect of water molecules on the structure, dynamics, and mechanical properties of sodium aluminosilicate hydrate (NASH) gel: a molecular dynamics study, Construct. Build. Mater. 193 (2018) 491-500.
[33] A.C. Van Duin, A. Strachan, S. Stewman, Q. Zhang, X. Xu, W.A. Goddard, ReaxFFSiO reactive force field for silicon and silicon oxide systems, J. Phys. Chem. A 107 (2003) 3803–3811.
[34] M.A. Qomi, K. Krakowiak, M. Bauchy, K. Stewart, R. Shahsavari, D. Jagannathan, D.B. Brommer, A. Baronnet, M.J. Buehler, S. Yip, Combinatorial molecular optimization of cement hydrates, Nat. Commun. 5 (2014) 4960.
[35] Y. Yu, B. Wang, M. Wang, G. Sant, M. Bauchy, Reactive molecular dynamics simulations of sodium silicate glasses—toward an improved understanding of the structure, Int. J. Appl. Glas. Sci. 8 (3) (2017) 276–284.
[36] R. Dongol, L. Wang, A. Cormack, S. Sundaram, Molecular dynamics simulation of sodium aluminosilicate glass structures and glass surface-water reactions using the reactive force field (ReaxFF), Appl. Surf. Sci. 439 (2018) 1103–1110.
[37] D.-C. Yue, T.-B. Ma, Y.-Z. Hu, J. Yeon, A.C. van Duin, H. Wang, J. Luo, Tribochemistry of phosphoric acid sheared between quartz surfaces: a reactive molecular dynamics study, J. Phys. Chem. C 117 (48) (2013) 25604–25614.
[38] D.-C. Yue, T.-B. Ma, Y.-Z. Hu, J. Yeon, A.C. van Duin, H. Wang, J. Luo, Tribochemical mechanism of amorphous silica asperities in aqueous environment: a reactive molecular dynamics study, Langmuir 31 (4) (2015) 1429–1436.
[39] K.L. Joshi, G. Psofogiannakis, A.C. Van Duin, S. Raman, Reactive molecular simulations of protonation of water clusters and depletion of acidity in H-ZSM-5 zeolite, Phys. Chem. Chem. Phys. 16 (34) (2014) 18433–18441.
[40] G.M. Psofogiannakis, J.F. McCleerey, E. Jaramillo, A.C. Van Duin, ReaxFF reactive molecular dynamics simulation of the hydration of Cu-SSZ-13 zeolite and the formation of Cu dimers, J. Phys. Chem. C 119 (12) (2015) 6678–6686.

[41] M.C. Pitman, A.C. Van Duin, Dynamics of confined reactive water in smectite clay–zeolite composites, J. Am. Chem. Soc. 134 (6) (2012) 3042–3053.
[42] J.L. Suter, L. Kabalan, M. Khader, P.V. Coveney, Ab initio molecular dynamics study of the interlayer and micropore structure of aqueous montmorillonite clays, Geochim. Cosmochim. Acta 169 (2015) 17–29.
[43] M. Meo, M. Rossi, Prediction of Young's modulus of single wall carbon nanotubes by molecular-mechanics based finite element modelling, Compos. Sci. Technol. 66 (11) (2006) 1597e1605.
[44] A. Bagheri, A. Nazari, J.G. Sanjayan, P. Rajeev, W. Duan, Fly ash-based boroaluminosilicate geopolymers: experimental and molecular simulations, Ceram. Int. 43 (5) (2017) 4119–4126.
[45] A-T. Akono, Fracture behavior of metakaolin-based geopolymer reinforced with carbon nanofibers, Ceram. Int J Ceramic Eng Sci. 2020;2:234–242.
[46] P. Jittabut, S. Horpibulsuk, Physical and microstructure properties of geopolymer nanocomposite reinforced with carbon nanotubes, Mater. Today:. Proc. 17 (2019) 1682–1692.
[47] M. Hassanzadeh-Aghdam, M. Mahmoodi, R. Ansari, Creep performance of CNT polymer nanocomposites -An emphasis on viscoelastic interphase and CNT agglomeration, Composites Part B 168, 2019, 274–281.
[48] M. Hasanzadeh, R. Ansari, M.K. Hassanzadeh-Aghdam, Evaluation of effective properties of piezoelectric hybrid composites containing carbon nanotubes, Mechanics of Materials 129, 2019 63–79.
[49] J. Lu, M. Luo, B.I. Yakobson, Glass composites reinforced with silicon-doped carbon nanotubes, Carbon 128 (2018) 231–236.
[50] N.V. Medhekar, A. Ramasubramaniam, R.S. Ruoff, V.B. Shenoy, Hydrogen bond networks in graphene oxide composite paper: structure and mechanical properties, ACS Nano 4 (4) (2010) 2300–2306.
[51] Q. Pei, Y. Zhang, V. Shenoy, A molecular dynamics study of the mechanical properties of hydrogen functionalized graphene, Carbon 48 (3) (2010) 898–904.

Tables

Table 1: Chemical composition of metakaolin geopolymer.

Si/Al ratio	*SiO_2 (wt%)*	*Al_2O_3 (wt%)*	*Na_2O (wt%)*	*H_2O (wt%)*	*Density (g/cm^3)*
3	48.60	27.40	16.30	7.70	2.00

Table 2: Diffusion coefficients of pristine CNT, CNT-oxide and Na^+ cations in CNT/geopolymer matrix.

Component	Diffusion coefficient 10^{-11} (m^2/s)	Other calculations 10^{-11} (m^2/s)
Pristine CNT	0.051	
CNT-oxide	0.166	
Na^+	0.376 (pristine CNT) 1.113 (CNT-oxide)	0.345 [26]

Figure captions

Figure 1: CNT/geopolymer model. The cyan, blue, green, red, yellow, white and orange spheres represent Si, Al, Na, O, H and C atoms, respectively.

Figure 2: (a) Atomic structure of Pristine (6,6) carbon nanotube, and (b) 10% doped CNT-oxide.

Figure 3: Variation of elastic modulus of CNT/geopolymer nanostructure with pristine CNT concentration.

Figure 4: Indentation modulus of CNT/geopolymer versus pristine CNT dosage.

Figure 5: Bulk density of the nanostructure as a function with CNT concentration.

Figure 6: Interfacial energy variation with CNT content.

Figure 7: Young modulus of CNT and CNT-oxide with various doping concentrations.

Figure 8: Unit cell of 10% doped CNT-oxide/geopolymer: (a) side view structure; (b) cross section structure showing the multiple links between CNT and geopolymer matrix; (c) zoom in perspective view of the nanostructure, where the C atoms connect with O atoms in the geopolymer structure (yellow Si, blue Al, green Na, red O, white H, grey-blue C).

Figure 9: Elastic modulus of functionalized CNT/geopolymer as function of doping CNT-oxide concentrations.

Figure 10: Effect of doping CNT-oxide dosage variation on the bulk density of functionalized CNT/geopolymer.

Figure 11: Mean Square Displacement of (a) pristine and functionalized CNT component and (b) Na^+ cation versus time simulation.

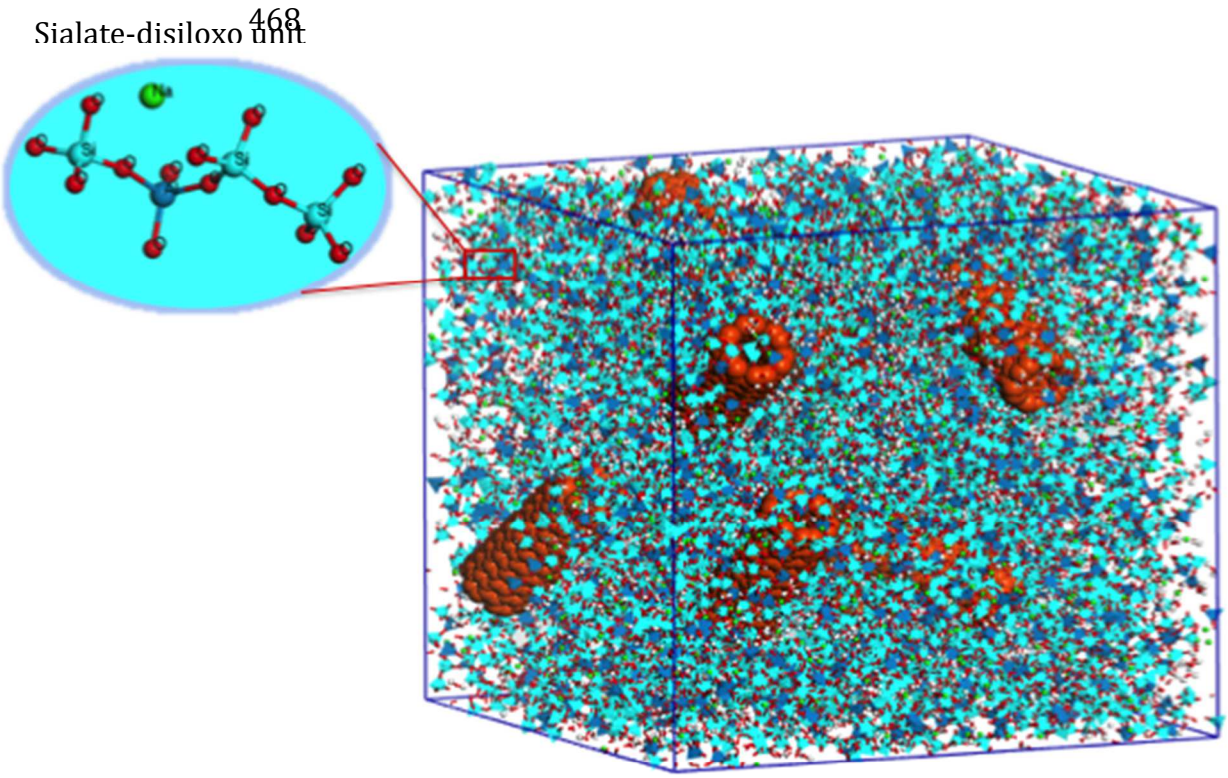

Figure 1

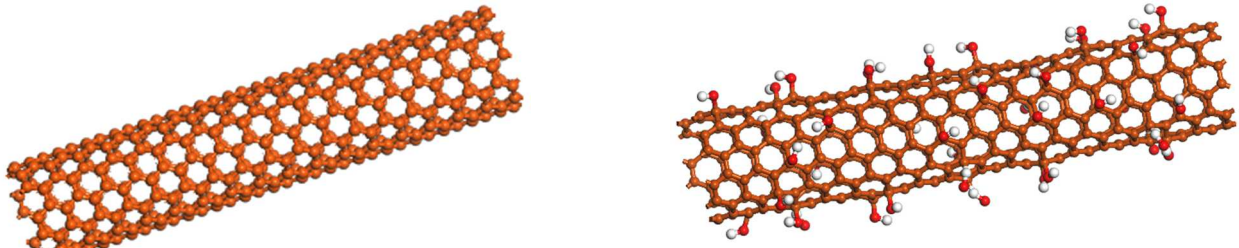

(a) (b)

Figure 2

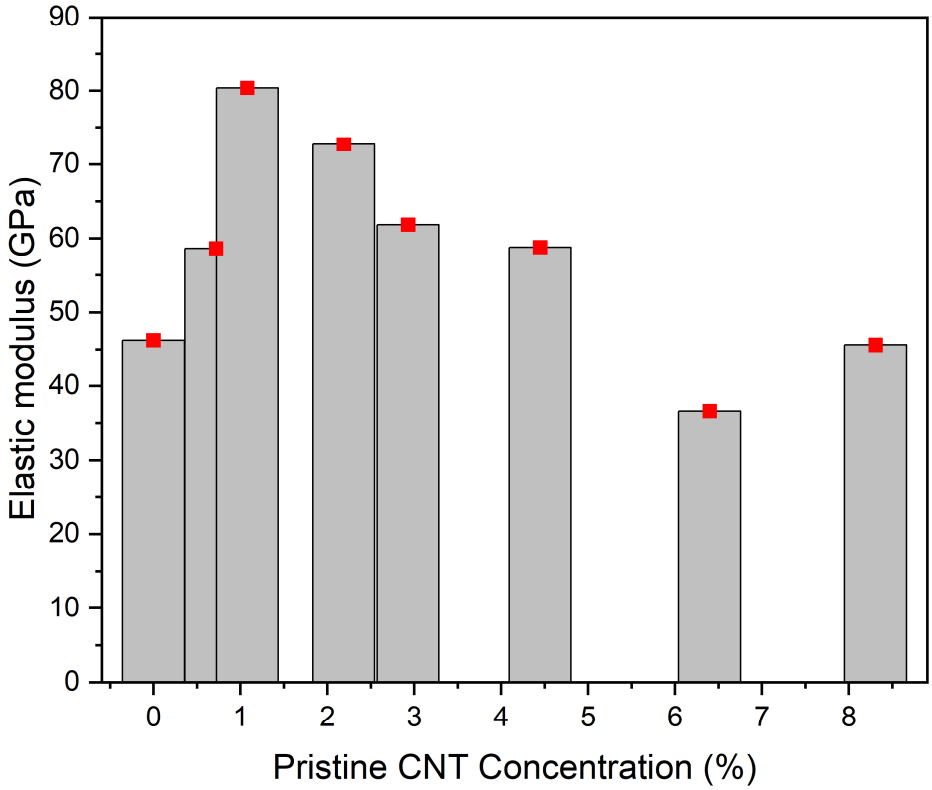
Elastic modulus (GPa)
0
10
20
30
40
50
60
70
80
90
0
1
2
3
4
5
6
7
8
Pristine CNT Concentration (%)

Figure 3

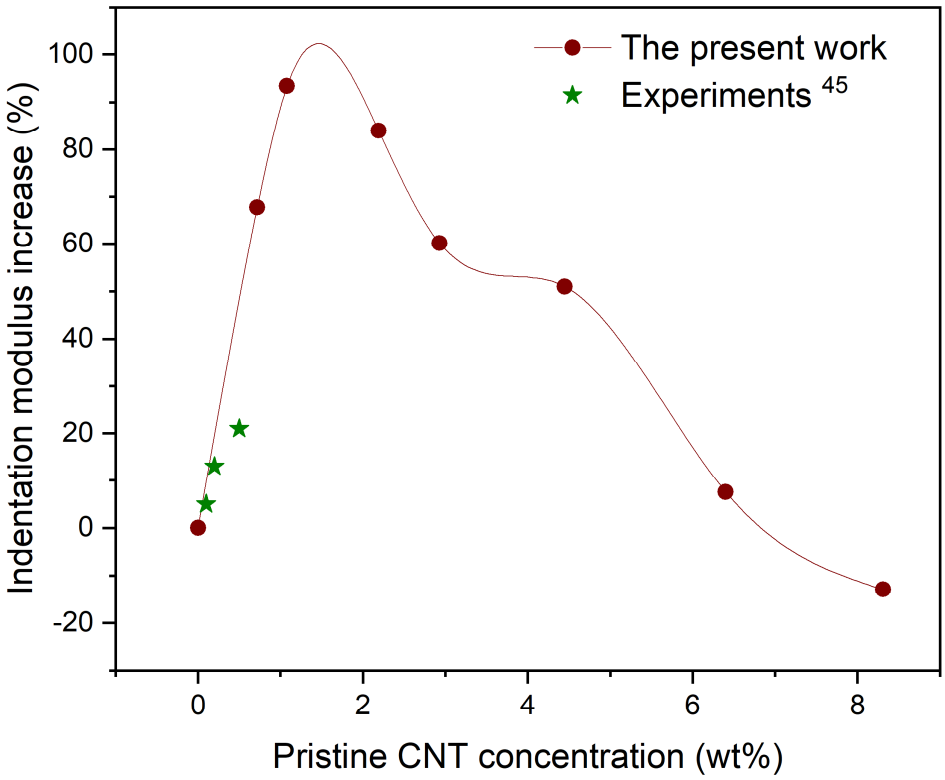
The present work
Experiments [45]
Indentation modulus increase (%)
Pristine CNT concentration (wt%)
100
80
60
40
20
0
-20
0
2
4
6
8

Figure 4

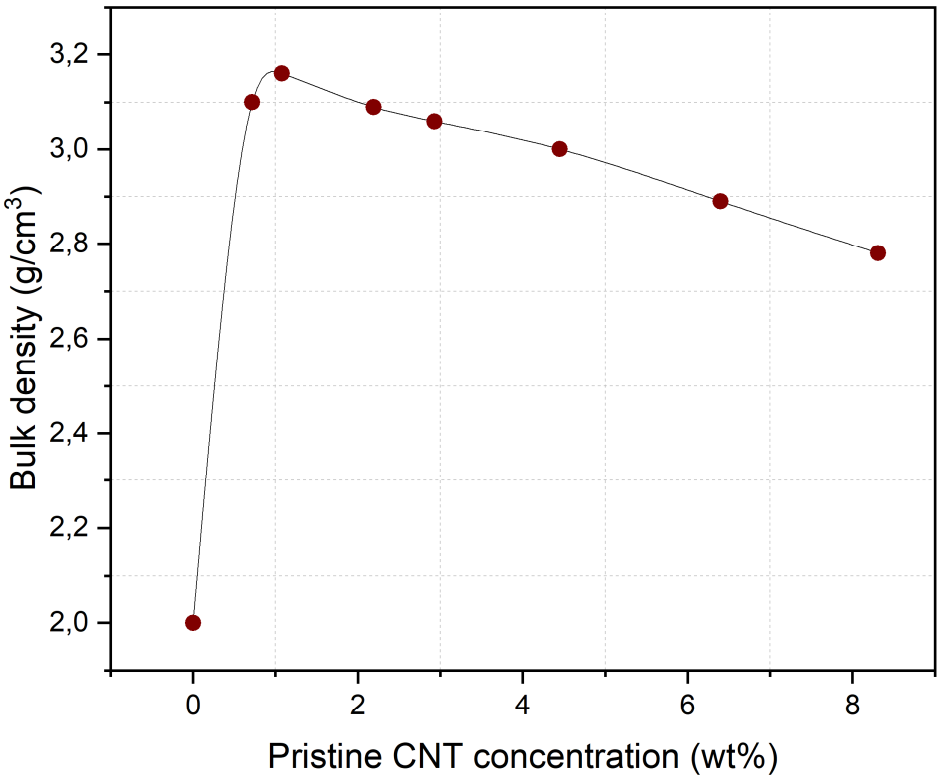

539
540
541
542
543 Figure 5
544
545
546
547
548
549

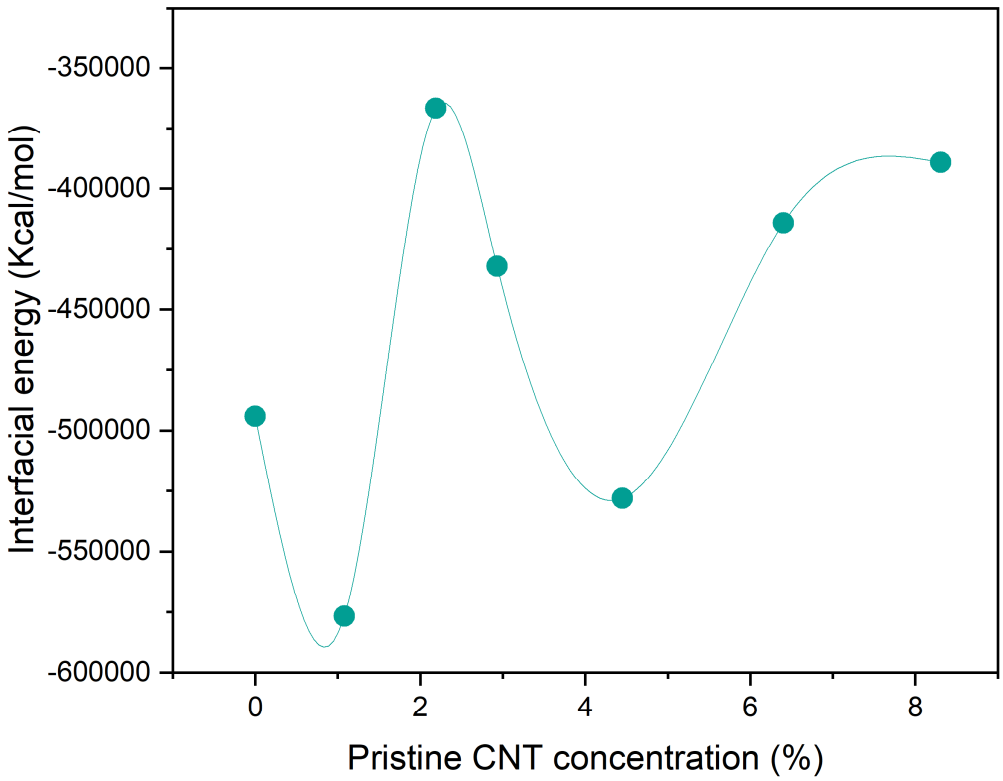
-350000
-400000
-450000
-500000
-550000
-600000
Interfacial energy (Kcal/mol)
0
2
4
6
8
Pristine CNT concentration (%)

Figure 6

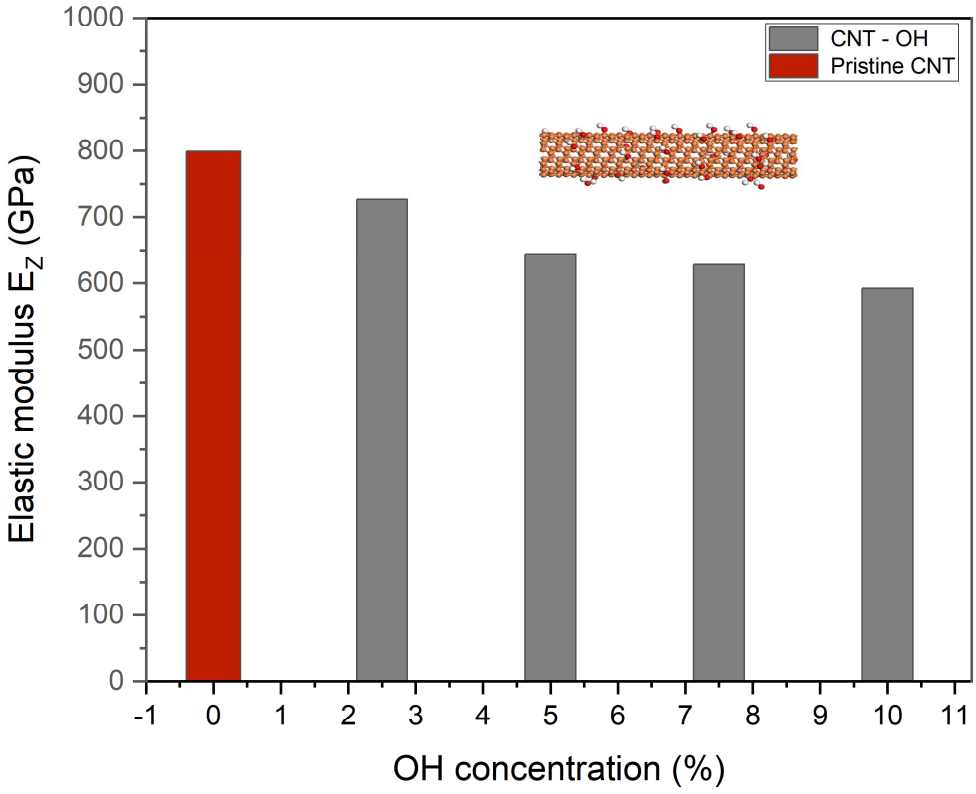
CNT - OH
Pristine CNT
Elastic modulus E_Z (GPa)
OH concentration (%)
0
100
200
300
400
500
600
700
800
900
1000
-1
0
1
2
3
4
5
6
7
8
9
10
11

Figure 7

(a) (b)

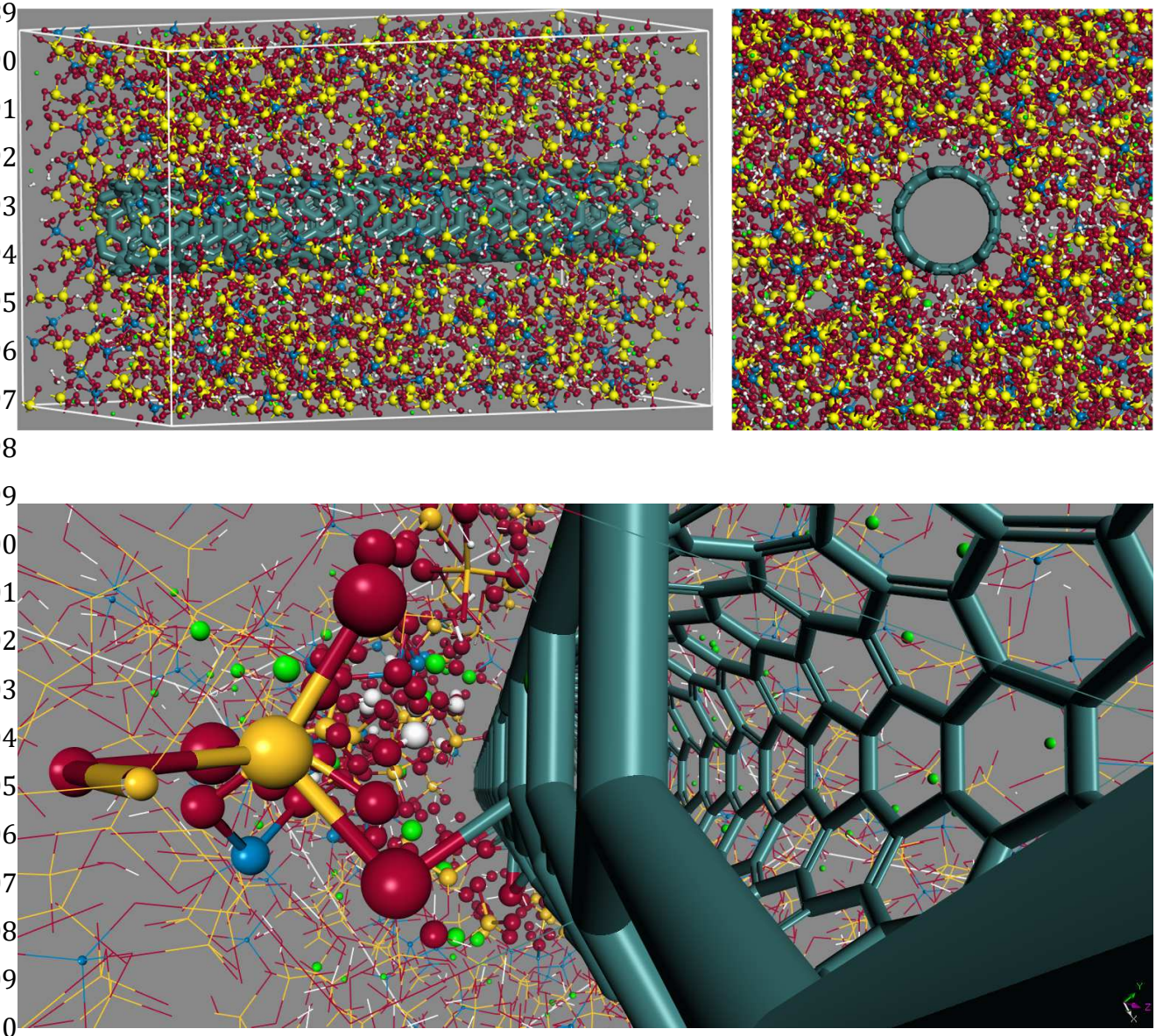

(c)

Figure 8

620

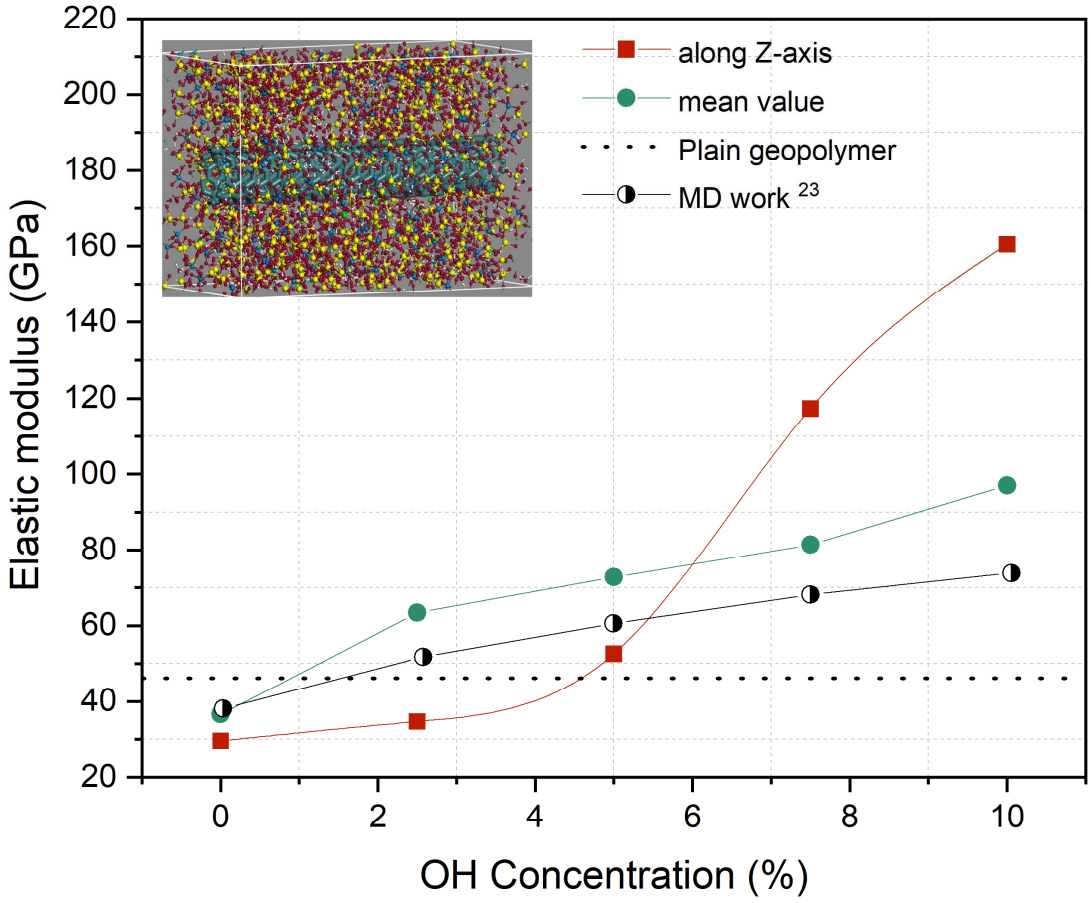

621

622

623

624 Figure 9

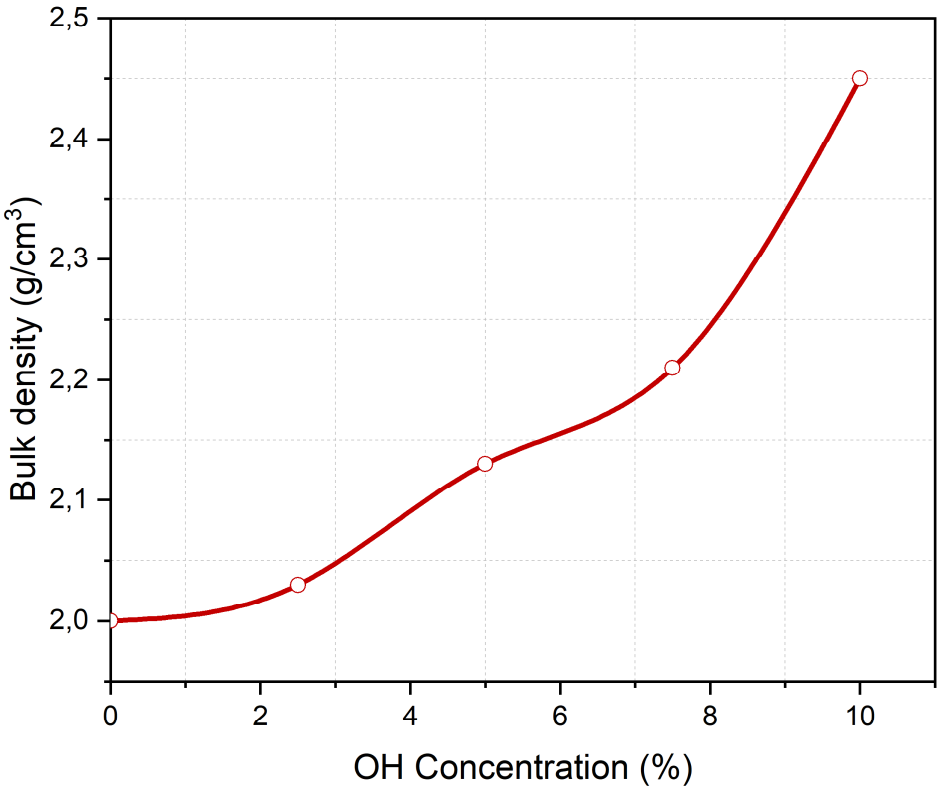

Figure 10

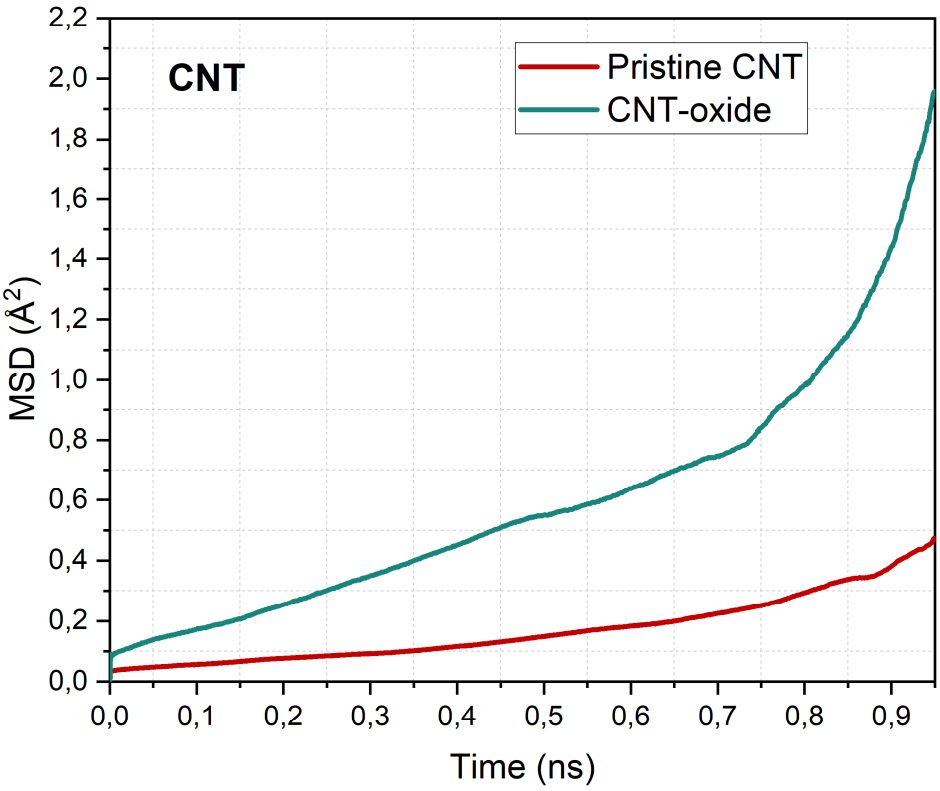
CNT
Pristine CNT
CNT-oxide
MSD (Å²)
Time (ns)
0,0
0,2
0,4
0,6
0,8
1,0
1,2
1,4
1,6
1,8
2,0
2,2
0,1
0,3
0,5
0,7
0,9

(a)

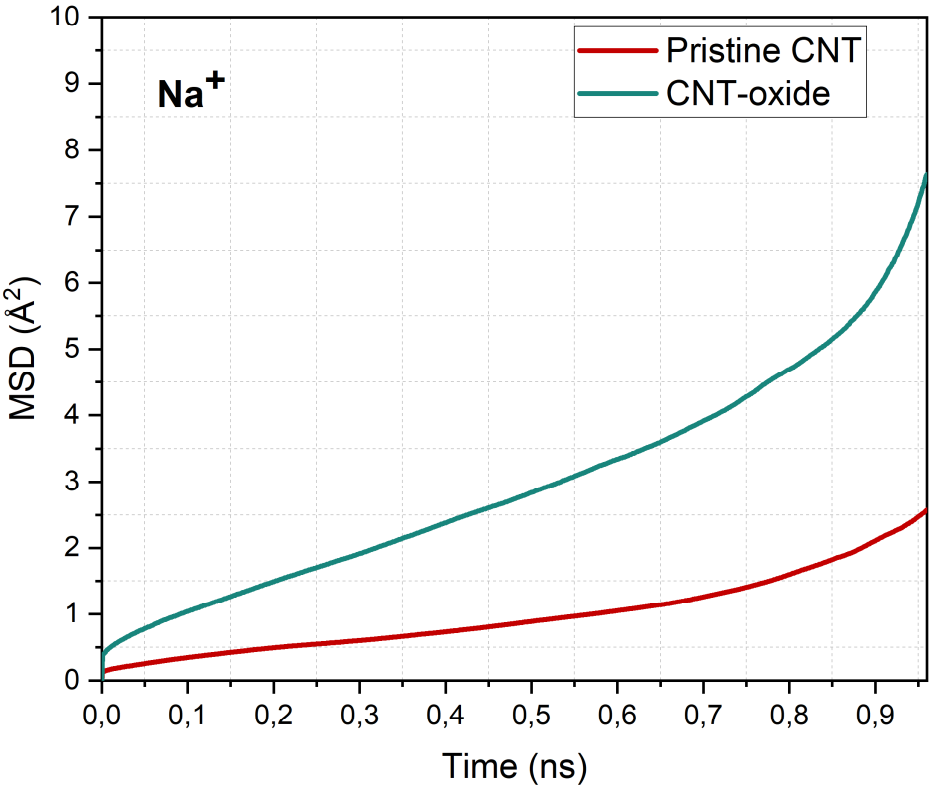
Na+
Pristine CNT
CNT-oxide
MSD (Å²)
Time (ns)
0
1
2
3
4
5
6
7
8
9
10
0,0
0,1
0,2
0,3
0,4
0,5
0,6
0,7
0,8
0,9

(b)

Figure 11

CNT/geopolymer nanostructure

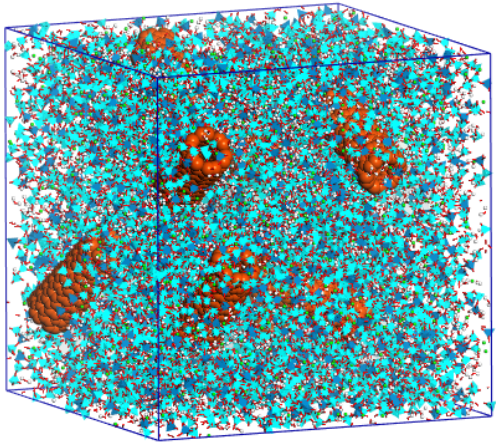

Enhancement up to 74%

Optimum CNTconcentration

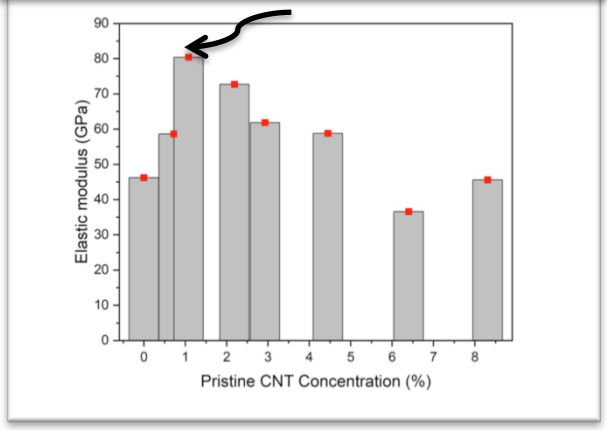

Functional CNT/geopolymer

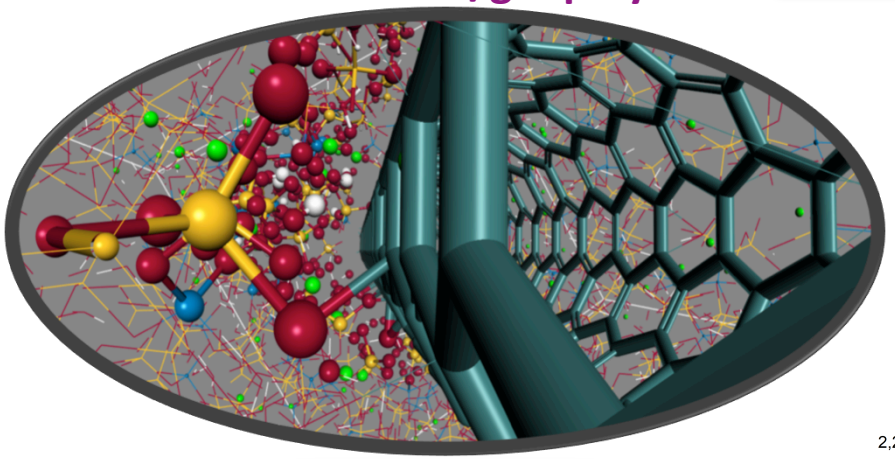

Mechanical properties

A raise of 165%

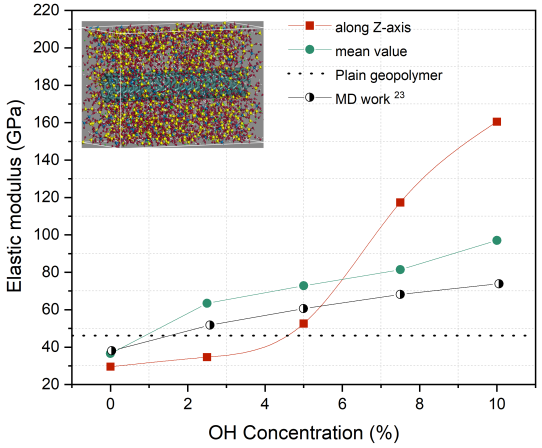

Dynamical properties

Faster CNT diffusion